YALE JOURNAL OF BIOLOGY AND MEDICINE 90 (2017), pp.25-33.

ORIGINAL CONTRIBUTION

YJBM

Variable Effects of Autophagy Induction by Trehalose on Herpesviruses Depending on Conditions of Infection

Jeffery L. Meier[a] and Charles Grose[b,*]

[a]*Virology laboratories, Department of Internal Medicine, University of Iowa, Iowa City, IA;* [b]*Department of Pediatrics, University of Iowa, Iowa City, IA*

Trehalose is a non-reducing sugar formed from two glucose units. Trehalose induces abundant autophagy in cultured cells and also reduces the rate of aggregation of the huntingtin protein in the animal model of Huntington disease, a chronic neurological disease in humans. The mechanism of this effect on autophagy is now known to be caused by starvation secondary to inhibition of a family of glucose transporters known as the solute carrier 2 or the glucose transporter family. Variable effects of trehalose treatment have been observed during infections with two herpesviruses—human cytomegalovirus and varicella-zoster virus. The reasons for differing results have now been delineated. These differences are caused by two variables in conditions of infection: timing of addition of trehalose and type of inoculum (cell-free virus vs. infected cells). When monolayers pretreated with trehalose were inoculated with cell-free virus, there was a decline in virus spread by as much as 93 percent when compared with untreated monolayers. However, when monolayers were inoculated with infected cells rather than cell-free virus, there was no decline in virus spread. These results demonstrated that the effect of trehalose was limited to monolayers that were starved when inoculated with cell-free virus. In contrast, sufficient virus was already present in infected cell inocula so as to minimize any inhibitory effect of a starved monolayer. These results also showed that trehalose did not specifically inhibit a herpesvirus; rather, addition of trehalose to cell culture media altered the intracellular environment.

INTRODUCTION

In this report, we re-investigate the effects of autophagy induction by trehalose on the infectious cycles of two human herpesviruses. Trehalose is a nonreducing sugar formed from two glucose units joined by a natural alpha-linked bond [1,2]. The effect of trehalose on inducing autophagy was initially documented in a mouse model of Huntington disease [3]. Huntington disease is caused by an abnormally long cytosine-adenine-guanine (CAG) trinucleotide repeat sequence in the *huntingtin* gene. Trehalose treatment reduced aggregation of a huntingtin construct in mice and also reduced cell death caused by huntingtin protein in cultured cells [4]. Trehalose treatment by itself significantly increased autophagosome levels in autophagy-competent Atg5-positive murine cells but not in autophagy-deficient Atg5-negative cells.

*To whom all correspondence should be addressed: Dr. Charles Grose, University of Iowa Children's Hospital, 200 Hawkins Drive, Iowa City IA 52242, Tel: 319-356-2270, Charles-grose@uiowa.edu.

†Abbreviations: HCMV, human cytomegalovirus; VZV, varicella-zoster virus; HSV, herpes simplex virus; Atg, autophagy protein; MAb, monoclonal antibody; MAP1LC3, microtubule-associated protein 1 light chain 3; PFU, plaque forming units.

Keywords: trehalose, autophagy, MAP1LC3, herpes simplex virus, cytomegalovirus, varicella-zoster virus, varicella vaccine

Author Contributions: JLM designed the CMV experiments and CG designed the VZV experiments. Both authors reviewed the data, then wrote and edited the final manuscript.

Copyright © 2017

The family of nine human herpesviruses has been divided into three subfamilies designated as alpha, beta, and gamma. We have previously observed that infection with the human alpha herpesvirus varicella-zoster virus (VZV†) leads to increased autophagic flux, while inhibition of autophagy leads to diminished viral spread [5-7]. Unlike the closely related herpes simplex virus (HSV), the VZV genome harbors no known inhibitors of autophagy, such as the HSV *ICP34.5* gene [8-10]. Based on the reports that trehalose induced autophagy, we postulated that the addition of trehalose to infected monolayers may facilitate the VZV infectious cycle [3]. Because VZV titers in infected cultures are so low, transfer of infectivity is generally carried out with trypsin-dispersed VZV-infected cells rather than cell free virus [11,12]. As an indicator of increased virus assembly in newly infected cultures, the production of the predominant structural VZV glycoprotein gE is an easily detectable marker by immunolabeling or immunoblotting [13]. When monolayers were inoculated with infected cells and allowed to incubate for 3 days, production of virions, as gauged by quantity of VZV gE in a density-gradient purified band, was modestly increased in cultures subsequently treated with medium containing trehalose [7].

In contrast to this positive effect of trehalose during the VZV infectious cycle, a recent paper about human cytomegalovirus (HCMV) reported an opposite result [14]. HCMV is a beta herpesvirus, which has a much larger genome than either HSV or VZV. The HCMV genome contains an inhibitor of autophagy that is not a homolog of HSV *ICP34.5* [15]. Addition of trehalose to medium overlying HCMV-infected cultures induced autophagy but reduced HCMV spread and titers of cell free virus. Because of these apparent divergent results, we re-investigated the effects of trehalose on both VZV and HCMV infections in cell culture.

MATERIALS AND METHODS

Cytomegalovirus

The clinical-like TB40/E strain of HCMV has a green fluorescent protein (GFP) gene driven by SV40 promoter, which is expressed during the early/late phase of infection [16,17]. The HCMV strain was maintained in the human retinal pigmented cell line ARPE-19 and subsequently amplified in human foreskin fibroblasts [18]. Culture medium overlying an infected fibroblast monolayer was collected and passed through a 0.45 uM pore filter. Virus present in the filtrate was further purified through a 20 percent sorbitol cushion gradient, after which the virus-containing pellet was re-suspended in medium with 50 percent newborn calf serum for storage at -80C. Monolayers were plated in 6-well culture cluster flat bottom dishes (Costar); after confluence, monolayers were inoculated with virus for 90 minutes under previously described conditions of infection [19].

Varicella-zoster Virus

The vaccine strain (vOka) was grown in MRC-5 monolayers until cytopathology was about 75 percent [20]. Unlike HCMV, VZV never releases cell-free virus from infected monolayers into culture media [21]. To obtain virus inocula by which to transfer VZV infectivity, two different methods were used [12]. For the first method, to obtain infected cells, monolayers were treated with trypsin-ethylenediaminetetraacidic solution to dislodge cells from the plastic surface. The individual infected cells were suspended in culture medium with 8 percent fetal calf serum and then transferred onto fresh monolayers at a ratio of one infected cell for every 8 uninfected cells [11]. The infected cells then attach to the uninfected cells during a 2 hour incubation and VZV infectivity is transferred without any release of cell-free virus into the medium. For the second method, to obtain cell-free virus, infected monolayers were dislodged with a rubber policeman into 2 ml of culture medium in a 12 ml plastic tube. The cell suspension was sonicated for 10 seconds as previously described [12]. After a low-speed sedimentation to remove debris, the cell-free virus in the supernatant was layered onto fresh monolayers. Titers of infected cells were 100,000 infectious centers/ml and titers of cell-free virus were 10,000 plaque-forming units (PFU)/ml. As with HCMV, all VZV infections were carried out in 6-well culture dishes.

Antibody Reagents

Murine MAbs against HCMV IE1/2 and CMV ICP8 (UL57) were purchased from Virusys Corporation (cat. # P1215 and P1209). These same two antibodies were used in an earlier investigation of trehalose treatment during CMV infection [14]. Murine MAb 3B3 against the VZV glycoprotein gE (ORF68) and MAb 5C6 against the VZV regulatory protein IE62 (ORF62) were produced in this laboratory; these antibody reagents have been extensively characterized, including the affinity of binding of MAb 3B3 to its gE linear epitope [22]. A rabbit antibody against the microtubule-associated protein 1 light chain 3 (MAP1LC3) protein was purchased from Sigma (cat. # L7543). Fluoroprobes included goat anti-mouse Alexa Fluor 546, goat anti-rabbit Alexa Fluor 488 as well as the Hoechst 33342 DNA stain (405 nm; Life Technologies).

Imaging and Quantitation by Confocal Microscopy

Procedures for confocal microscopy of virus-infected monolayers with application of the Imaris software program for 3D animation have been extensively described by this laboratory [6,23,24]. Imaging of virus-in-

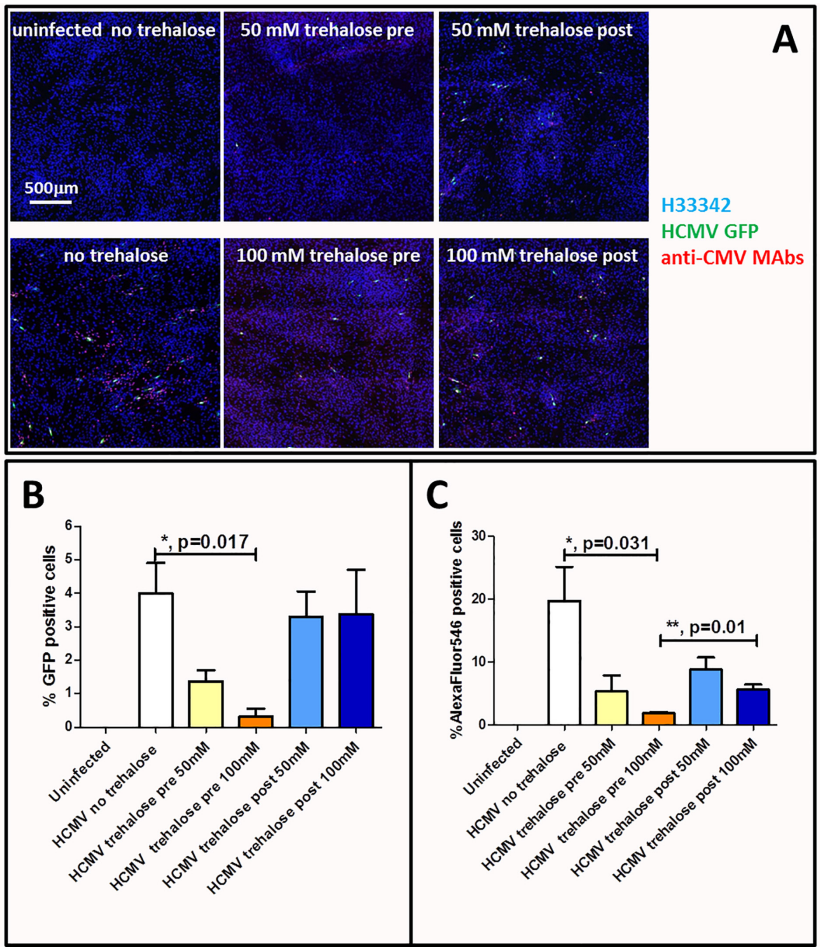

Figure 1. Effect of trehalose on HCMV infection. A. Confocal micrographs of monolayers under different conditions of HCMV infection. **B.** Graph of GFP-positive cells in monolayer under 6 conditions: uninfected cells without trehalose, infected cells without trehalose, infected with 50 mM trehalose added 16 hr before virus inoculation, infected cells with 100 mM trehalose added 16 hr before virus inoculation, infected cells with 50 mM trehalose added at same time as virus inoculation, infected cells with 100 mM trehalose added at same time as virus inoculation. **C.** Graph of infected cells positive after staining with mixture of two anti-HCMV MAbs under six conditions: uninfected cells without trehalose, infected cells without trehalose, infected with 50 mM trehalose added 16 hr before virus inoculation, infected cells with 100 mM trehalose added 16 hr before virus inoculation, infected cells with 50 mM trehalose added at same time as virus inoculation, infected cells with 100 mM trehalose added at same time as virus inoculation.

fected and uninfected monolayers was performed with an upright Zeiss LSM710 spectral confocal microscope, using 10X, 20X, 40X, and 63X objective lenses. The confocal pinhole was assigned to 1 Airy unit. Image size was set to 1024 x 1024 pixels for conventional imaging and 512 x 512 pixels for acquisition of multiple images within a z-stack. Excitation was via four lasers: 405 nm, 488 nm, 561 nm and 633 nm. Images were analyzed using proprietary Zen software (Zeiss) and National Institutes of Health ImageJ software [25]. The pixel intensity was quantitated using ImageJ software by the following method: images were opened in ImageJ in a single channel and converted to a 32-bit image, after which the Measure tool in the Analysis menu was used to obtain an average pixel intensity [23]. The ratio of the pixel intensity of each protein to the Hoechst 33342 pixel intensity was then calculated for each tile image. Graphs were created from the pixel data with GraphPad Prism software and presented as column bar graphs. The standard error of the mean across each set of images was used to generate error bars. *P* values were determined by unpaired, two-tailed Student's *t* tests. Levels of statistical significance in the graphs are demarcated as follows: not significant = $p > 0.05$; * = < 0.05 ; ** = < 0.01; *** = < 0.001.

RESULTS

Effects of Trehalose on HCMV Infection

Trehalose treatment was found previously to inhibit

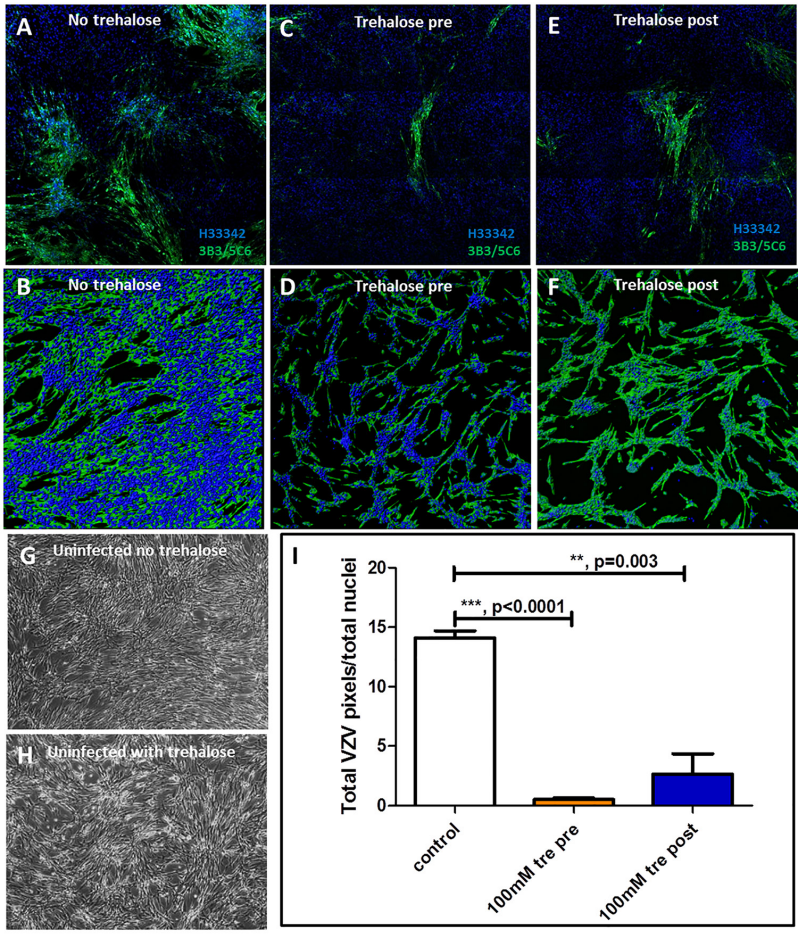

Figure 2. Effect of trehalose after inoculation of monolayers with VZV cell-free virus. A. Visualization of the monolayers after fixation was carried out by conventional confocal microscopy and subsequently by rendering a z-stack of 2D images into a 3D animation by Imaris software. **A,B.** Representative 2D and 3D images of VZV infected cells four days after infection in the absence of trehalose. VZV proteins gE and IE62 are immunolabeled (green); nuclei are blue. **C,D.** Representative 2D and 3D images of VZV infected monolayers treated with 100 mM trehalose 16 hr before inoculation. VZV gE is immunolabeled. **E,F.** Representative 2D and 3D images of VZV infected monolayers treated with trehalose at time of inoculation. VZV gE is immunolabeled. **G.** Uninfected cells in the absence of trehalose. **H.** Uninfected cells treated with trehalose for four days. **I.** Graph of total VZV gE-positive pixels/total nuclei.

HCMV spread [14]. In an initial set of experiments, we duplicated the protocol of HCMV experiments carried out in a previous publication; we also added another time-point that included addition of trehalose-containing medium 16 hours before inoculation with virus. Monolayers of fibroblasts were inoculated with cell free virus at a multiplicity of infection of 0.025 PFU/cell. The monolayers were incubated for 3 days, after which the infected monolayers were fixed and incubated with a mixture of the 2 anti-HCMV MAbs followed by secondary fluoroprobes. When viewed by confocal microscopy, it was apparent by both the patterns of 488 nm (GFP) and 546 nm (MAbs) fluorescent immunolabeling that pretreatment with trehalose for 16 hours prior to virus inoculation reduced HCMV spread (Figure 1A). Results were assayed in cultures with only fluorescent labeled virus (Figure 1B) and in cultures in which a mixture of 2 anti-CMV antibodies was added to the cultures post-fixation to enhance detection of infectious foci (Figure 1C). The decreased spread as enumerated by the number of CMV-positive cells following trehalose pretreatment (100 mM) was statistically significant when compared with no trehalose treatment under both sets of immunolabeling conditions ($p = 0.017$; $p = 0.031$). The percent decrease in spread ranged from 80 percent (Figure 1B) to 93 percent (Figure 1C). The decrease in spread was not significant with pretreatment with 50 mM trehalose (Figure 1B,C). When trehalose was added at the same time as the virus inoculum, the spread was reduced but not to a level of statistical significance (Figure 1B,C). We also observed that quantitation of foci with anti-HCMV MAb probes delineated a significant de-

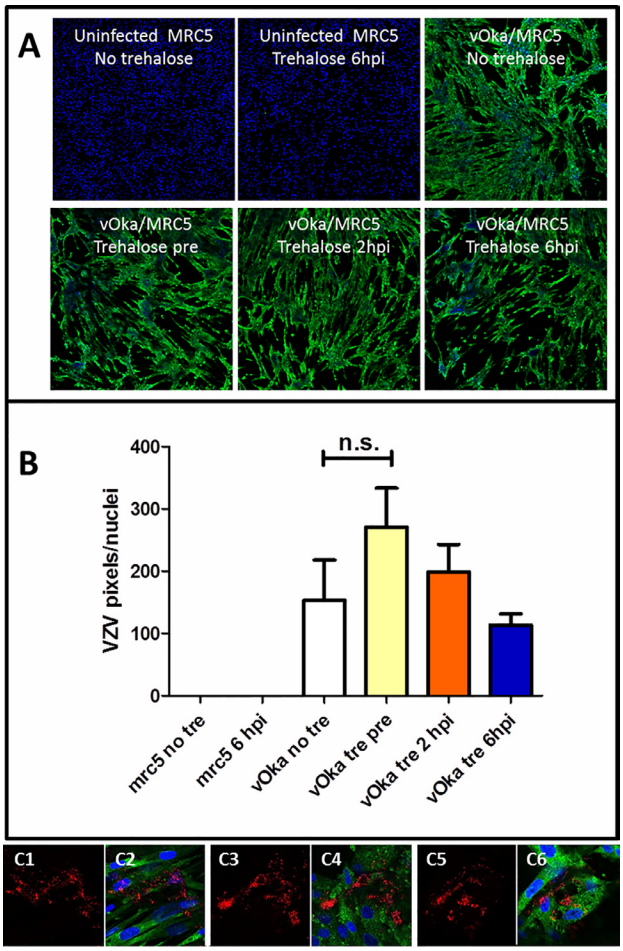

Figure 3. Effect of trehalose after inoculation of monolayers with VZV infected cells. A. Confocal microscopy. The six panels include the following conditions: Uninfected cells without trehalose, uninfected cells with trehalose added after 6 hr, infected cells without trehalose, infected cells with trehalose added 16 hr before infection, infected cells with trehalose added 2 hr after infection and infected cells with trehalose added 6 hr after infection. Both VZV gE and IE62 proteins were labeled to demarcate spread of virus (green). **B.** Graph of VZV gE-positive pixels/nuclei after varying conditions described in panel A. **C.** Confocal microscopy to show effect of trehalose on VZV spread and autophagosome production. The left panel of each pair shows VZV gE alone and the merged right panel shows gE and LC3. C1-2: infection without addition of trehalose; C3-4: infection after pretreatment with trehalose; C5-6: infection followed by trehalose treatment after 6 hr. VZV gE = red; MAP1LC3 = green; DNA stain = blue.

crease in number of foci ($p = 0.01$) between infected cultures pretreated with 100 mM trehalose compared with infected cultures treated with 100 mM trehalose at time of infection (Figure 1C).

Effects of Trehalose After Inoculation of Monolayers with VZV Cell-free Virus

To more closely compare the above results with HCMV infections carried out with cell-free virus, similarly timed experiments were carried out with VZV cell-free virus. Since there is no release of cell-free virus from VZV-infected monolayers, VZV cell free virus was prepared by sonic disruption of infected cells as described in Methods. Because of the low titer of input virus, these monolayers were incubated for 4 days after infection. The monolayers were fixed and analyzed after imaging by confocal microscopy; the analysis included conversion of z-stacks into 3D animations by Imaris software. The results showed decreased VZV spread in the presence of trehalose as compared with no trehalose treatment: inoculation with cell-free virus without trehalose (Figure 2A,B); addition of trehalose 16 hours before virus inoculation (Figure 2C,D) or addition at the same time as virus inoculation (Figure 2E,F). Control experiments are included in Figure 2G,H. As shown in the graph in Figure 2I, the reduction in spread was highly significant after quantitation by described methods for both trehalose pretreatment ($p = < 0.0001$) and post-treatment ($p = 0.003$). These VZV results were similar to the HCMV results in Figure 1.

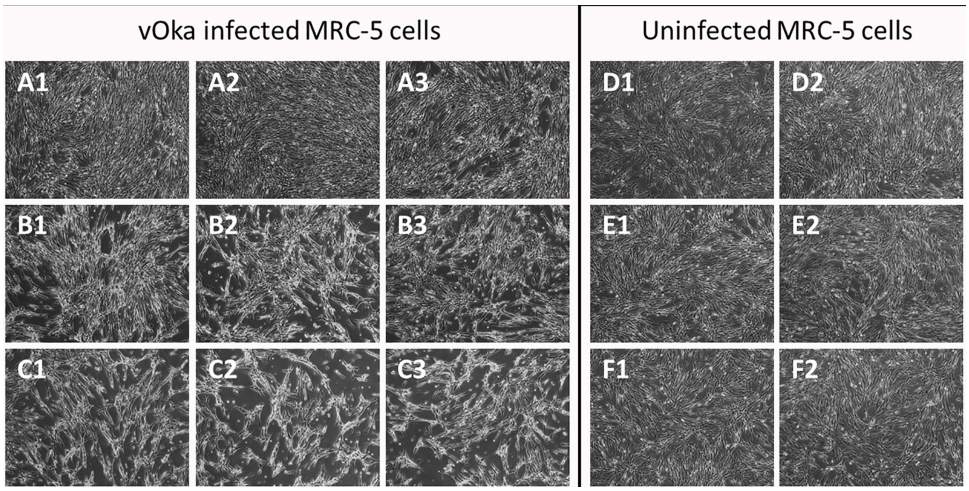

Figure 4. Effect of trehalose on cytopathic effect induced by VZV infection. All cultures were observed after incubation for 72 hr under the described conditions of infection. **A.** Three representative panels of VZV infected monolayers in the absence of trehalose. **B.** Three representative panels of VZV infected monolayers treated with 50 mM trehalose. **C.** Three representative panels of VZV infected monolayers treated with 100 mM trehalose. **D.** Duplicate control panels of uninfected monolayers in the absences of trehalose. **E.** Duplicate control uninfected monolayers treated with 50 m trehalose. **F.** Duplicate control uninfected monolayers treated with 100 mM trehalose.

Effects of Trehalose after Inoculation of Monolayers with VZV-infected Cells

Because of the results with VZV cell-free virus, we repeated the experiments to assess the effect of trehalose treatment on VZV spread after inoculation with trypsin-dispersed VZV-infected cells. This experiment complemented the experiment that was previously described in an earlier VZV publication [7]. Because of the higher titer of input virus in the infected cells, these monolayers were incubated for 3 days after inoculation (Figure 3). In this experiment, trehalose was added 16 hours before infection, 2 hours after infection or 6 hours after infection (Figure 3A). Trehalose cannot be added at the same time as infection, because the infected-cell inoculum is layered onto the uninfected monolayer for 2 hours and then removed. The results with trehalose were different than those shown in Figure 2. Namely, with an inoculum of infected cells, there was no significant difference in VZV spread under any condition of trehalose pretreatment or post-treatment when compared with infection without trehalose treatment (Figure 3B). In a separate trehalose experiment, we immunolabeled a second set of monolayers similarly inoculated with VZV-infected cells with both murine antibody to VZV gE and rabbit antibody to the MAP1LC3 protein, in order to assess the degree of VZV spread together with autophagosome formation, under conditions without trehalose treatment or with trehalose treatment before and after infection (Figure 3C). By confocal microscopy, we found similar VZV spread as well as abundant autophagy under all three conditions in which monolayers were inoculated with VZV-infected cells.

Effects of Trehalose on Virus-induced Cytopathic Effect

We also observed subtle signs of toxicity related to trehalose in infected monolayers beginning on day 3 of treatment (Figure 4). When the degree of virus-induced cytopathic effect in treated infected cells was compared with untreated infected cells, it was apparent that trehalose treatment of an infected monolayer was increasing slightly the degree of virus-induced cytopathic effect (Figure 4). In particular, after 72 hours of 100 mM trehalose treatment of infected monolayers, there were larger gaps in the monolayers (Figure 4C2 and 4C3) that were not seen in untreated but infected monolayers (Figure 4A2 and 4A3). By comparison, gaps were not seen in uninfected control monolayers treated with 100 mM trehalose for 72 hours (Figure 4F).

DISCUSSION

The 2016 Nobel Prize for Medicine or Physiology was awarded to Professor Yoshinori Ohsumi for his pioneering research on mechanisms of autophagy [26,27]. Autophagy is a process by which proteins and organelles within a cell are recycled [28,29]. As shown in Figure 5, the autophagy pathway in human cells includes a series of compartments and related autophagy (Atg) proteins. The pathway begins in the endoplasmic reticulum (ER) with the formation of the omegasome, which undergoes a step-wise transition to the double-walled autophagosome. Misfolded and damaged cytoplasmic proteins are engulfed within the autophagosome [30]. The autophagosome is characterized by the presence in its wall of

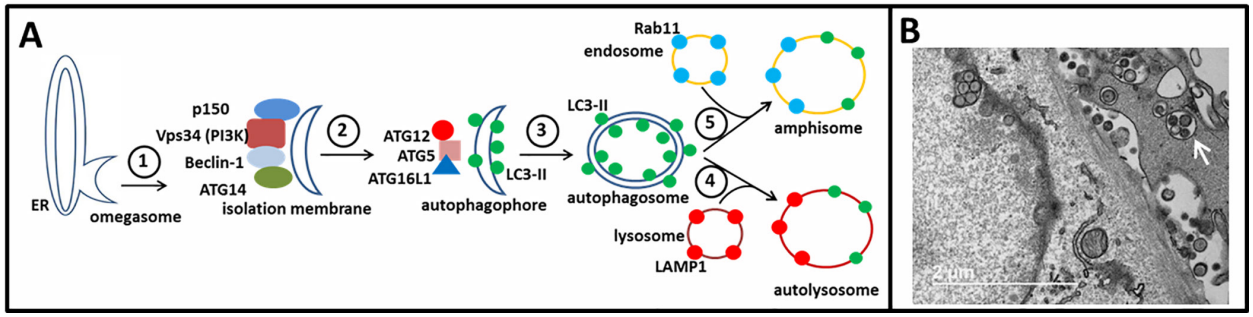

Figure 5. Diagram of the autophagy pathway in mammalian cells. A. Autophagy pathway. An initial step in autophagy includes the transition from an omegasome to an isolation membrane (step 1). The viral protein HSV ICP34.5 interferes with step 2. Autophagosomes have a characteristic double outer wall containing the LC3-II protein (step 3). Conventional autophagy includes step 4 as the conclusion of autophagic flux. Fusion of an autophagosome with an endosome leads to a single-walled amphisome (step 5). **B.** Electron micrograph of VZV infected cells. There are several single walled vesicles in the cytoplasm that contain between 1 to 4 viral particles (arrow). We have proposed that some vesicles have properties resembling an amphisome [41]. Viral particles are not seen in double-walled vesicles.

the MAP1LC3B-II (MAP1LC3B-II, or simply LC3B-II protein), which is a lipidated form of LC3B-I; LC3 is a mammalian homolog of Saccharomyces cerevisiae Atg8 [31]. Subsequently, the autophagosome can fuse with an endosome to form an amphisome or fuse with a lysosome to form an autolysosome [32,33]. In the latter situation, lysosomal enzymes degrade the cargo and recycle the peptides (autophagic flux). Since invasion of a cell by a virus is a stressful event, virus infection must accommodate itself to autophagy. Autophagy has been observed and studied following infection with both RNA and DNA viruses [34-38].

The biochemical mechanism by which trehalose induces autophagy was reported recently. Trehalose inhibits a family of glucose transporters known as the solute carrier 2 (SLC2A) or the glucose transporter (GLUT) family [39]. Thus, treatment with trehalose creates a starved cell and starvation leads to increased autophagosome formation within the cell as a survival strategy. This effect may be mediated through the AMPK signaling pathway or by mTORC1 suppression or possibly through MPK-mTORC1 crosstalk. As shown in this report, the effect of trehalose on herpesvirus infection of cultured cells depends on two factors: (i) timing of addition of trehalose and (ii) type of inoculum: cell-free virus versus infected cells. Inoculation with cell-free virus (either HCMV or VZV) onto monolayers that have been pretreated with trehalose for 16 hours leads to little or no spread of infection. Inoculation with cell-free virus (either HCMV or VZV) onto monolayers that have trehalose added at the same time as virus inoculation leads to a major reduction in spread. This latter result confirms the data presented in the earlier report about the effect of trehalose on CMV spread [14]. The prior CMV report also noted that the inhibitory effects of trehalose were not dependent on a particular cell substrate in which CMV was propagated. All these results are compatible with a hypothesis that growth of a cell-free herpesvirus (either HCMV or VZV) is restricted after entering a cell that is starved secondary to trehalose treatment. Note that there may be some confusion in terminology between HCMV and VZV investigations because cell-free HCMV obtained from sonication of infected cells is called "infected cell virus" while cell-free VZV obtained from sonication of infected cells is called "cell free virus." We avoided the use of the term "infected cell virus" for CMV virus in this report.

With regard to VZV specifically, the point of most interest is that the inhibitory effect of trehalose on virus spread is not apparent when the inoculum consists of infected cells rather than cell-free virus. Again, we point out that VZV infected cells do not release cell-free virus after they are layered onto an uninfected monolayer; most likely, virus is transferred from infected to uninfected cell after fusion of the outer membrane of an infected cell to an uninfected cell. We had previously demonstrated that trehalose treatment may increase the production of the major gE glycoprotein in the virion fraction. In that experiment, trehalose was added 6 hours after inoculation of monolayers with infected cells. In light of the new data in Figure 4 of this report, we modify our previous conclusion to state that VZV gE levels and autophagy levels may have been increased, but probably not to a statistically significant degree. Nevertheless, based on the data in Figure 4, we also emphasize that VZV replication within infected cells was not inhibited by trehalose treatment. We now postulate that there is sufficient virus within infected cells that is sufficiently advanced in its replication cycle, so that the enhancing effects of trehalose-induced autophagy on new virus formation can equalize or even outweigh the deleterious effects of trehalose-induced starvation on the underlying monolayer.

In two recent publications, we further defined a po-

tential role for autophagy in the VZV infectious cycle [40,41]. We have previously documented that specific inhibition of autophagosome formation by ATG5 siRNA reduced VZV spread [7]. This observation raised the possibility that autophagic membranes may be involved in viral spread. Subsequently, we showed that some newly assembled VZ virions were enclosed within single-walled vesicles with attributes of an amphisome [40]. As shown in Figure 5A, an amphisome is formed by fusion of an autophagosome with an endosome; an amphisome contains two distinctive markers: LC3 (autophagy pathway) and Rab11 (endosomal pathway). Our data suggest that during or immediately following secondary virion envelopment in the virus assembly compartment, some virions are enclosed in and transported to the cell surface within a vesicle with both LC3 and Rab11 marker proteins (Figure 5B). Therefore, any enhanced production of autophagosomes secondary to treatment of infected cells with trehalose would facilitate increased formation of amphisomes or amphisome-like vesicles. Further research will be required to define more detailed contributions of the autophagy pathway to VZV assembly and trafficking. Moreover, a recent publication describing enhanced autophagy during replication of a second alpha herpesvirus (duck enteritis virus) in a pattern very similar to VZV suggests that inhibition of autophagy is not the norm for most alpha herpesviruses outside of the two HSV-1 and HSV-2 species [42].

Our conclusions are limited because we currently have no methodology by which to isolate and purify the cytoplasmic vesicles which contain the viral particles. Presumably, purification would require a series of density gradient centrifugations. If these vesicles could be purified free from all other cellular membranes and organelles, we could enumerate and compare the number of vesicles under the different conditions of infection with and without trehalose; also, we could verify the components of the outer wall of the vesicles and thereby determine if the vesicles that carry newly assembled virions were a homogenous population.

Acknowledgments: CG received post-doctoral training in glycobiology from Professor Elbein (1933-2009), who authored references 1 and 2 in this report. This research project was supported by NIH grant AI89716 (CG).

REFERENCES

1. Elbein AD. The metabolism of alpha,alpha-trehalose. Adv Carbohydr Chem Biochem. 1974;30:227-56.
2. Elbein AD, Pan YT, Pastuszak I, Carroll D. New insights on trehalose: a multifunctional molecule. Glycobiology. 2003;13(4):17R-27R.
3. Sarkar S, Davies JE, Huang Z, Tunnacliffe A, Rubinsztein DC. Trehalose, a novel mTOR-independent autophagy enhancer, accelerates the clearance of mutant huntingtin and alpha-synuclein. J Biol Chem. 2007;282(8):5641-52.
4. Rubinsztein DC, Bento CF, Deretic V. Therapeutic targeting of autophagy in neurodegenerative and infectious diseases. J Exp Med. 2015;212(7):979-90.
5. Carpenter JE, Jackson W, Benetti L, Grose C. Autophagosome formation during varicella-zoster virus infection following endoplasmic reticulum stress and the unfolded protein response. J Virol. 2011;85(18):9414-24.
6. Buckingham EM, Carpenter JE, Jackson W, Zerboni L, Arvin AM, Grose C. Autophagic flux without a block differentiates varicella-zoster virus infection from herpes simplex virus infection. Proc Natl Acad Sci U S A. 2015;112(1):256-61.
7. Buckingham EM, Carpenter JE, Jackson W, Grose C. Autophagy and the effects of its inhibition on varicella-zoster virus glycoprotein biosynthesis and infectivity. J Virol. 2014;88(2):890-902.
8. Grose C, Buckingham EM, Jackson W, Carpenter JE. The pros and cons of autophagic flux among herpesviruses. Autophagy. 2015;11(4):716-7.
9. Orvedahl A, Alexander D, Talloczy Z, Sun Q, Wei Y, Zhang W, et al. HSV-1 ICP34.5 confers neurovirulence by targeting the Beclin 1 autophagy protein. Cell Host Microbe. 2007;1(1):23-35.
10. Horien C, Grose C. Neurovirulence of varicella and the live attenuated varicella vaccine virus. Semin Pediatr Neurol. 2012;19(3):124-9.
11. Grose C, Perrotta DM, Brunell PA, Smith GC. Cell-free varicella-zoster virus in cultured human melanoma cells. J Gen Virol. 1979;43(1):15-27.
12. Grose C, Brunel PA. Varicella-zoster virus: isolation and propagation in human melanoma cells at 36 and 32 degrees C. Infect Immun. 1978;19(1):199-203.
13. Olson JK, Bishop GA, Grose C. Varicella-zoster virus Fc receptor gE glycoprotein: serine/threonine and tyrosine phosphorylation of monomeric and dimeric forms. J Virol. 1997;71(1):110-9.
14. Belzile JP, Sabalza M, Craig M, Clark E, Morello CS, Spector DH. Trehalose, an mTOR-Independent Inducer of Autophagy, Inhibits Human Cytomegalovirus Infection in Multiple Cell Types. J Virol. 2016;90(3):1259-77.
15. Chaumorcel M, Lussignol M, Mouna L, Cavignac Y, Fahie K, Cotte-Laffitte J, et al. The human cytomegalovirus protein TRS1 inhibits autophagy via its interaction with Beclin 1. J Virol. 2012;86(5):2571-84.
16. Sinzger C, Hahn G, Digel M, Katona R, Sampaio KL, Messerle M, et al. Cloning and sequencing of a highly productive, endotheliotropic virus strain derived from human cytomegalovirus TB40/E. J Gen Virol. 2008;89(Pt 2):359-68.
17. O'Connor CM, Murphy EA. A myeloid progenitor cell line capable of supporting human cytomegalovirus latency and reactivation, resulting in infectious progeny. J Virol. 2012;86(18):9854-65.
18. Meier JL, Stinski MF. Effect of a modulator deletion on transcription of the human cytomegalovirus major immediate-early genes in infected undifferentiated and differentiated cells. J Virol. 1997;71(2):1246-55.
19. Yuan J, Li M, Torres YR, Galle CS, Meier JL. Differentiation-Coupled Induction of Human Cytomegalovirus Replication by Union of the Major Enhancer Retinoic Acid,

Cyclic AMP, and NF-kappaB Response Elements. J Virol. 2015;89(24):12284-98.
20. Gomi Y, Sunamachi H, Mori Y, Nagaike K, Takahashi M, Yamanishi K. Comparison of the complete DNA sequences of the Oka varicella vaccine and its parental virus. J Virol. 2002;76(22):11447-59.
21. Weller TH. Serial Propagation in vitro of agents producing inclusion bodies derived from varicella and herpes zoster. Proc Soc Exp Biol Med. 1953;83:340-6.
22. Grose C, Tyler S, Peters G, Hiebert J, Stephens GM, Ruyechan WT, et al. Complete DNA sequence analyses of the first two varicella-zoster virus glycoprotein E (D150N) mutant viruses found in North America: evolution of genotypes with an accelerated cell spread phenotype. J Virol. 2004;78(13):6799-807.
23. Jackson W, Yamada M, Moninger T, Grose C. Visualization and quantitation of abundant macroautophagy in virus-infected cells by confocal three-dimensional fluorescence imaging. J Virol Methods. 2013;193(1):244-50.
24. Buckingham EM, Carpenter JE, Jackson W, Grose C. Nuclear LC3-positive puncta in stressed cells do not represent autophagosomes. Biotechniques. 2014;57(5):241-4.
25. Schneider CA, Rasband WS, Eliceiri KW. NIH Image to ImageJ: 25 years of image analysis. Nat Methods. 2012;9(7):671-5.
26. Takeshige K, Baba M, Tsuboi S, Noda T, Ohsumi Y. Autophagy in yeast demonstrated with proteinase-deficient mutants and conditions for its induction. J Cell Biol. 1992;119(2):301-11.
27. Mizushima N, Noda T, Yoshimori T, Tanaka Y, Ishii T, George MD, et al. A protein conjugation system essential for autophagy. Nature. 1998;395(6700):395-8.
28. Yang Z, Klionsky DJ. Eaten alive: a history of macroautophagy. Nat Cell Biol. 2010;12(9):814-22.
29. Mizushima N, Yoshimori T, Ohsumi Y. The role of Atg proteins in autophagosome formation. Annu Rev Cell Dev Biol. 2011;27:107-32.
30. Choi AM, Ryter SW, Levine B. Autophagy in human health and disease. N Engl J Med. 2013;368(19):1845-6.
31. Kabeya Y, Mizushima N, Ueno T, Yamamoto A, Kirisako T, Noda T, et al. LC3, a mammalian homologue of yeast Apg8p, is localized in autophagosome membranes after processing. EMBO J. 2000;19(21):5720-8.
32. Klionsky DJ, Eskelinen EL, Deretic V. Autophagosomes, phagosomes, autolysosomes, phagolysosomes, autophagolysosomes... wait, I'm confused. Autophagy. 2014;10(4):549-51.
33. Sanchez-Wandelmer J, Reggiori F. Amphisomes: out of the autophagosome shadow? EMBO J. 2013;32(24):3116-8.
34. Dreux M, Gastaminza P, Wieland SF, Chisari FV. The autophagy machinery is required to initiate hepatitis C virus replication. Proc Natl Acad Sci U S A. 2009;106(33):14046-51.
35. Alirezaei M, Flynn CT, Whitton JL. Interactions between enteroviruses and autophagy in vivo. Autophagy. 2012;8(6):973-5.
36. Kudchodkar SB, Levine B. Viruses and autophagy. Rev Med Virol. 2009;19(6):359-78.
37. Jackson WT. Viruses and the autophagy pathway. Virology. 2015;479-480:450-6.
38. Moreau P, Moreau K, Segarra A, Tourbiez D, Travers MA, Rubinsztein DC, et al. Autophagy plays an important role in protecting Pacific oysters from OsHV-1 and Vibrio aestuarianus infections. Autophagy. 2015;11(3):516-26.
39. DeBosch BJ, Heitmeier MR, Mayer AL, Higgins CB, Crowley JR, Kraft TE, et al. Trehalose inhibits solute carrier 2A (SLC2A) proteins to induce autophagy and prevent hepatic steatosis. Sci Signal. 2016;9(416):ra21.
40. Buckingham EM, Jarosinski KW, Jackson W, Carpenter JE, Grose C. Exocytosis of Varicella-Zoster Virus Virions Involves a Convergence of Endosomal and Autophagy Pathways. J Virol. 2016;90(19):8673-85.
41. Grose C, Buckingham EM, Carpenter JE, Kunkel JP. Varicella-Zoster Virus Infectious Cycle: ER Stress, Autophagic Flux, and Amphisome-Mediated Trafficking. Pathogens. 2016;5(4):E67
42. Zhao L, Yin HC, Li SQ, Niu YJ, Jiang XJ, Xu LJ, et al. Autophagy Activated by Duck Enteritis Virus Infection Positively Affects Its Replication. J Gen Virol. 2016; Epub ahead of print.